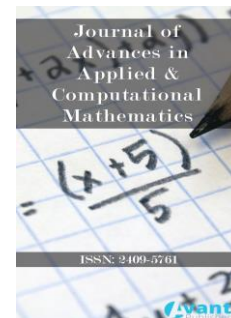




Published by Avanti Publishers  
**Journal of Advances in Applied &  
Computational Mathematics**

ISSN (online): 2409-5761



---

## The Electromagnetic Scattering Problem by a Cylindrical Doubly-Connected Domain at Oblique Incidence: An Inverse Problem


Leonidas Mindrinos \*

Department of Natural Resources Development and Agricultural Engineering, Agricultural University of Athens, Athens 118 55, Greece

---

### ARTICLE INFO

Article Type: Research Article

Academic Editor: Zui-Cha Deng 

Keywords:

Inverse problem

Electromagnetic scattering

Singular integral equations

Timeline:

Received: June 08, 2023

Accepted: July 15, 2023

Published: August 07, 2023

Citation: Mindrinos L. The electromagnetic scattering problem by a cylindrical doubly-connected domain at oblique incidence: An inverse problem. J Adv App Comput Math. 2023; 10: 18-25.

DOI: <https://doi.org/10.15377/2409-5761.2023.10.2>

### ABSTRACT

In this work, we examine the inverse problem to reconstruct the inner boundary of a cylindrical doubly-connected infinitely long medium from measurements of the scattered electromagnetic wave in the far-field. We consider the integral representation of the solution to derive a non-linear system of equations for the unknown radial function. We propose an iterative scheme using linearization and regularization techniques.

---

\*Corresponding Author

Email: [leonidas.mindrinos@aua.gr](mailto:leonidas.mindrinos@aua.gr)

Tel: +(30) 2105294117

## 1. Introduction

Inverse scattering problems are a class of applied mathematical problems that arise in various fields, such as medical imaging, radar technology, and non-destructive testing. These problems involve the reconstruction of an unknown scatterer (its geometry and/or material properties) from the measurements of the scattered waves close or far from the medium. We refer to the textbooks [1-3] for the fundamentals and an extensive overview.

In the special case of obliquely incident scattering problems, where the incident wave is not normal (perpendicular) to the scatterer or the boundary, additional complexity is introduced. The scattering events depend on the incident angle and thus such problems pose additional theoretical and numerical challenges compared to normal incidence. The analysis of these problems often involves advanced mathematical and computational approaches to account for the increased complexity, see for example the early works [4, 5].

However, if we specify the scatterer to be infinitely long and spatial-independent in one direction then the three-dimensional problem reduces to a set of two-dimensional problems and the complexity has to do only with the boundary conditions where the tangential derivative of the fields appear. Motivated by the works of Nakamura and Wang, see for example [6, 7], we examined scattering problems for penetrable simply- and doubly-connected scatterers [8, 9].

In this work, we are interested in solving numerically the inverse problem to reconstruct the inner boundary curve of a doubly connected penetrable infinitely long cylinder with impedance-type conditions in its inner boundary. The well-posedness of the corresponding direct problem was proven by the author in [10].

We formulate the inverse problem as a system of singular boundary integral equations to be solved for the unknown density functions, see the initial work of Kress and Rundell [11]. The radial function appears non-linearly and we apply the Fréchet derivative on the integral operator. The ill-posedness is treated with Tikhonov regularization.

The paper is organized as follows: In `sec_direct` we formulate the direct problem and we present the necessary differential equations, boundary, and radiation conditions. The inverse problem and the equivalent system of integral equations are stated in `sec_inverse` where we propose also the numerical iterative scheme for its solution. In the last section, we present the numerical implementation and numerical examples justifying the applicability of the proposed method.

## 2. Problem Formulation

In [10] the author considered the direct scattering problem of a time-harmonic electromagnetic wave by an infinitely long, penetrable, and doubly-connected cylinder. The initial problem is stated in 3D but the properties of the medium allow for an equivalent formulation in 2D for the cross-section of the scatterer. The medium is bounded by two disjoint smooth boundaries. We impose transmission conditions on the exterior and Leontovich impedance conditions on the inner boundary.

Let  $\Omega_1$  denote the horizontal cross-section of the cylindrical scatterer, with a smooth boundary  $\Gamma$ , consisting of two disjoint closed curves  $\Gamma_1$  (inner) and  $\Gamma_0$  (outer) such that  $\Gamma = \Gamma_1 \cup \Gamma_0$ . The exterior domain is denoted by  $\Omega_0$ .

We define the wave-number  $\kappa_j^2 = \mu_j \varepsilon_j \omega^2 - \beta^2$ , for  $j = 0, 1$  where  $\mu_j$  and  $\varepsilon_j$  are the material parameters and  $\beta = k_0 \cos \theta$ , where  $k_0 = \omega \sqrt{\mu_0 \varepsilon_0}$ , for the frequency  $\omega$  and  $\theta \in (0, \pi)$  is the incident angle concerning the negative  $z$ -axis.

Following [6-8, 10], the direct problem is governed by the Helmholtz equations

$$\begin{aligned} \Delta e^{ext} + \kappa_0^2 e^{ext} &= 0, & \Delta h^{ext} + \kappa_0^2 h^{ext} &= 0, & \text{in } \Omega_0, \\ \Delta e^1 + \kappa_1^2 e^1 &= 0, & \Delta h^1 + \kappa_1^2 h^1 &= 0, & \text{in } \Omega_1, \end{aligned}$$

for the exterior  $e^{ext}, h^{ext}$  and the interior  $e^1, h^1$  electric and magnetic fields, respectively. The boundary conditions read

$$\begin{aligned}
 e^1 - e^{ext} &= 0, \quad \text{on } \Gamma_0, \\
 \tilde{\mu}_1 \omega \frac{\partial h^1}{\partial n} + \beta_1 \frac{\partial e^1}{\partial \tau} - \tilde{\mu}_0 \omega \frac{\partial h^{ext}}{\partial n} - \beta_0 \frac{\partial e^{ext}}{\partial \tau} &= 0, \quad \text{on } \Gamma_0, \\
 h^1 - h^{ext} &= 0, \quad \text{on } \Gamma_0, \\
 \tilde{\varepsilon}_1 \omega \frac{\partial e^1}{\partial n} - \beta_1 \frac{\partial h^1}{\partial \tau} - \tilde{\varepsilon}_0 \omega \frac{\partial e^{ext}}{\partial n} + \beta_0 \frac{\partial h^{ext}}{\partial \tau} &= 0, \quad \text{on } \Gamma_0, \\
 \tilde{\mu}_1 \omega \frac{\partial h^1}{\partial n} + \beta_1 \frac{\partial e^1}{\partial \tau} + \lambda i h^1 &= 0, \quad \text{on } \Gamma_1, \\
 \lambda \tilde{\varepsilon}_1 \omega \frac{\partial e^1}{\partial n} - \lambda \beta_1 \frac{\partial h^1}{\partial \tau} + i e^1 &= 0, \quad \text{on } \Gamma_1,
 \end{aligned}$$

where appear both the normal and tangential derivatives of the fields. The impedance function  $\lambda$  is known. Here, we used

$$\tilde{\mu}_j = \frac{\mu_j}{\kappa_j^2}, \quad \tilde{\varepsilon}_j = \frac{\varepsilon_j}{\kappa_j^2}, \quad \beta_j = \frac{\beta}{\kappa_j^2}, \quad \text{for } j = 0,1.$$

The exterior fields are written as the sum of the scattered  $e^0, h^0$  and incident fields  $e^{inc}, h^{inc}$ , given by

$$e^{inc}(\mathbf{x}) = \frac{1}{\sqrt{\varepsilon_0}} \sin \theta e^{i\kappa_0(x \cos \varphi + y \sin \varphi)}, \quad h^{inc}(\mathbf{x}) = 0, \quad \mathbf{x} = (x, y), \tag{1}$$

where  $\varphi$  is the polar angle of the incident direction. The scattered wave satisfies also the Sommerfeld radiation condition.

The direct problem admits a unique solution [10]. In this work, we are interested in solving numerically the inverse problem to reconstruct the boundary curve  $\Gamma_1$ , given  $\lambda$  and the far-field pattern  $e^\infty(\hat{\mathbf{x}}), h^\infty(\hat{\mathbf{x}})$  of the scattered field, for all  $\hat{\mathbf{x}}$  in the unit circle.

### 3. The Inverse Problem

Given the far-fields, we aim to reconstruct the inner boundary of the scatterer given its material parameters and the impedance function. To do so, we present the solution of the problem using its integral representation.

Thus, we define the single- and double-layer potentials

$$\begin{aligned}
 (S_{klj}f)(\mathbf{x}) &= \int_{\Gamma_j} \Phi_k(\mathbf{x}, \mathbf{y}) f(\mathbf{y}) ds(\mathbf{y}), \quad \mathbf{x} \in \Omega_l, \\
 (D_{klj}f)(\mathbf{x}) &= \int_{\Gamma_j} \frac{\partial \Phi_k}{\partial n(\mathbf{y})}(\mathbf{x}, \mathbf{y}) f(\mathbf{y}) ds(\mathbf{y}), \quad \mathbf{x} \in \Omega_l,
 \end{aligned}$$

for  $k, l, j = 0,1$ , where  $\Phi_k$  is the fundamental solution of the Helmholtz equation in  $R^2$ , and  $f$  is a continuous density function. In addition, we define the integral operators

$$\begin{aligned}
 (S_{klj}f)(\mathbf{x}) &= \int_{\Gamma_j} \Phi_k(\mathbf{x}, \mathbf{y}) f(\mathbf{y}) ds(\mathbf{y}), \quad \mathbf{x} \in \Gamma_l, \\
 (D_{klj}f)(\mathbf{x}) &= \int_{\Gamma_j} \frac{\partial \Phi_k}{\partial n(\mathbf{y})}(\mathbf{x}, \mathbf{y}) f(\mathbf{y}) ds(\mathbf{y}), \quad \mathbf{x} \in \Gamma_l,
 \end{aligned}$$

$$(NS_{klj}f)(\mathbf{x}) = \int_{\Gamma_j} \frac{\partial \phi_k}{\partial n(\mathbf{x})}(\mathbf{x}, \mathbf{y}) f(\mathbf{y}) ds(\mathbf{y}), \quad \mathbf{x} \in \Gamma_l,$$

$$(ND_{klj}f)(\mathbf{x}) = \int_{\Gamma_j} \frac{\partial^2 \phi_k}{\partial n(\mathbf{x}) \partial n(\mathbf{y})}(\mathbf{x}, \mathbf{y}) f(\mathbf{y}) ds(\mathbf{y}), \quad \mathbf{x} \in \Gamma_l,$$

$$(TS_{klj}f)(\mathbf{x}) = \int_{\Gamma_j} \frac{\partial \phi_k}{\partial \tau(\mathbf{x})}(\mathbf{x}, \mathbf{y}) f(\mathbf{y}) ds(\mathbf{y}), \quad \mathbf{x} \in \Gamma_l,$$

$$(TD_{klj}f)(\mathbf{x}) = \int_{\Gamma_j} \frac{\partial^2 \phi_k}{\partial \tau(\mathbf{x}) \partial n(\mathbf{y})}(\mathbf{x}, \mathbf{y}) f(\mathbf{y}) ds(\mathbf{y}), \quad \mathbf{x} \in \Gamma_l,$$

needed in the following analysis.

We apply both the direct and indirect methods and we consider a single-layer ansatz for the interior fields and a modified Green representation for the exterior fields. The exterior fields are represented through a combination of potentials where we have specified the density functions to reduce the number of unknowns.

We set

$$\begin{aligned} e^1(\mathbf{x}) &= (\mathcal{S}_{110}\psi_1^e)(\mathbf{x}) + (\mathcal{S}_{111}\psi_2^e)(\mathbf{x}), & \mathbf{x} \in \Omega_1, \\ h^1(\mathbf{x}) &= (\mathcal{S}_{110}\psi_1^h)(\mathbf{x}) + (\mathcal{S}_{111}\psi_2^h)(\mathbf{x}), & \mathbf{x} \in \Omega_1, \\ e^0(\mathbf{x}) &= (\mathcal{D}_{000}\varphi_0^e)(\mathbf{x}) + \frac{\tilde{\epsilon}_1}{\tilde{\epsilon}_0}(\mathcal{S}_{000}\psi_1^e)(\mathbf{x}), & \mathbf{x} \in \Omega_0, \\ h^0(\mathbf{x}) &= (\mathcal{D}_{000}\varphi_0^h)(\mathbf{x}) + \frac{\tilde{\mu}_1}{\tilde{\mu}_0}(\mathcal{S}_{000}\psi_1^h)(\mathbf{x}), & \mathbf{x} \in \Omega_0. \end{aligned} \quad (2)$$

Then, using the standard jump relations, we find that the fields (2) solve the boundary value problem if the densities satisfy a well-posed Fredholm-type system of integral equations. We enlarge the system with the sum of the two far-field equations, given the specific form of the scattered fields. In the end, we obtain the system

$$\mathbf{A}\boldsymbol{\varphi} = \mathbf{b}, \quad (3)$$

where

$$\mathbf{A} = \begin{pmatrix} 1 + A_{11} & 0 & 0 & A_{14} & 0 & A_{16} \\ 0 & 1 + A_{22} & A_{23} & A_{24} & A_{25} & A_{26} \\ 0 & A_{32} & 1 + A_{33} & 0 & A_{35} & 0 \\ A_{41} & A_{42} & 0 & 1 + A_{44} & A_{45} & A_{46} \\ 0 & A_{52} & 0 & A_{54} & 1 + A_{55} & A_{56} \\ 0 & A_{62} & 0 & A_{64} & A_{65} & 1 + A_{66} \\ D^\infty & \frac{\tilde{\mu}_1}{\tilde{\mu}_0} S^\infty & D^\infty & \frac{\tilde{\epsilon}_1}{\tilde{\epsilon}_0} S^\infty & 0 & 0 \end{pmatrix},$$

and  $\boldsymbol{\varphi} = (\varphi_0^e, \psi_1^h, \varphi_0^h, \psi_1^e, \psi_2^h, \psi_2^e)^T$  for the right-hand side  $\mathbf{b} = (-2e^{inc}, 0, 0, \frac{\tilde{\epsilon}_0}{\tilde{\epsilon}_1} \partial_n e^{inc}, 0, 0, e^\infty + h^\infty)^T$ . The elements (integral operators) of the matrix are given by

$$\begin{aligned}
 A_{11} &= A_{33} = 2D_{000}, & A_{16} &= A_{35} = -2S_{101}, \\
 A_{14} &= -2\left(S_{100} - \frac{\tilde{\varepsilon}_1}{\tilde{\varepsilon}_0}S_{000}\right), & A_{22} &= A_{44} = NS_{100} - NS_{000}, \\
 A_{23} &= -\frac{\tilde{\mu}_0}{\tilde{\mu}_1}ND_{000}, & A_{24} &= \frac{\beta_1 - \beta_0}{\tilde{\mu}_1\omega}TS_{100}, \\
 A_{25} &= A_{46} = NS_{101}, & A_{26} &= \frac{\beta_1 - \beta_0}{\tilde{\mu}_1\omega}TS_{101}, \\
 A_{32} &= -2\left(S_{100} - \frac{\tilde{\mu}_1}{\tilde{\mu}_0}S_{000}\right), & A_{41} &= -\frac{\tilde{\varepsilon}_0}{\tilde{\varepsilon}_1}ND_{000}, \\
 A_{42} &= \frac{\beta_0 - \beta_1}{\tilde{\varepsilon}_1\omega}TS_{100}, & A_{45} &= \frac{\beta_0 - \beta_1}{\tilde{\varepsilon}_1\omega}TS_{101}, \\
 A_{52} &= -2NS_{110} - \frac{2i\lambda}{\tilde{\mu}_1\omega}S_{110}, & A_{54} &= -\frac{2\beta_1}{\tilde{\mu}_1\omega}TS_{110}, \\
 A_{55} &= -2NS_{111} - \frac{2i\lambda}{\tilde{\mu}_1\omega}S_{111}, & A_{56} &= -\frac{2\beta_1}{\tilde{\mu}_1\omega}TS_{111}, \\
 A_{62} &= -\frac{2\beta_1}{\tilde{\varepsilon}_1\omega}TS_{110}, & A_{64} &= -2NS_{110} + \frac{2i}{\lambda\tilde{\varepsilon}_1\omega}S_{110}, \\
 A_{65} &= \frac{2\beta_1}{\tilde{\varepsilon}_1\omega}TS_{111}, & A_{66} &= -2NS_{111} + \frac{2i}{\lambda\tilde{\mu}_1\omega}S_{111}.
 \end{aligned}$$

Here,  $D^\infty$  and  $S^\infty$  denote the far-field operators of  $D_{000}$  and  $S_{000}$ , respectively, where we replace  $\Phi_0$  with its far-field approximation.

The system (3) has to be solved for the six unknown density functions and the parametrization of the interior boundary curve. We propose to split it into two sub-systems and use the iterative scheme proposed in [12] and further applied successfully in many inverse problems, see for example [9, 13-15]. The difference here is that the far-field equation does not provide information on  $\Gamma_1$ , so we have to consider this equation together with the boundary equations for recovering the density functions (ill-posed problem) and solve instead one boundary equation for the unknown boundary.

Let us write (3) in a row-based form

$$A[k]\boldsymbol{\varphi} = \mathbf{b}[k], \quad \text{for } k = 1, \dots, 7.$$

The iterative scheme reads: Given an initial guess for the radial function, solve the sub-system of equations for  $k = 2, \dots, 7$  for the six density functions. Then, replace the derived density functions and solve the linearized form of the equation  $A[1]\boldsymbol{\varphi} = \mathbf{b}[1]$  to obtain the update for the boundary. We could choose any equation to be solved for the radial function but in the first or the third equation only one operator involving the radial function of the inner boundary, thus, it will be easier to linearize.

We solve the linear system using Tikhonov regularization, meaning by minimizing the following functional

$$\|(A'_1[1]\boldsymbol{\varphi})\mathbf{q} - \mathbf{b}[1] - A[1]\boldsymbol{\varphi}\|_2^2 + \lambda\|\mathbf{q}\|_2^2, \quad \lambda > 0,$$

where  $A'_1[1]$  denotes the Fréchet derivative of the operator depending on  $\Gamma_1$  (specified in the next section) and  $\mathbf{q}$  the radial function (to be reconstructed). The regularization parameter is decreasing at every iteration step.

### 4. Numerical Examples

We assume star-like boundary curves of the form

$$\Gamma_j = r_j(t)(\cos t, \sin t): t \in [0, 2\pi], \quad j = 0, 1,$$

for a smooth radial function  $r_j$  and we consider an equidistant grid discretization  $t_k = k\pi/n$ , for  $k = 0, \dots, 2n - 1$ .

The discretized form of the operators are analytically presented In [10] and they are omitted here for the sake of presentation. We apply quadrature rules to handle the singular kernels. We present only the single layer and its Fréchet derivative.

We observe that only the operator  $S_{101}$  depends (non-linearly) on  $\Gamma_1$ , and it is explicitly given by

$$\begin{aligned} (S_{101}(r_1; \phi))(t) &= \int_0^{2\pi} \Phi_1(\mathbf{y}(t), \mathbf{x}(\tau)) \phi(\tau) |\mathbf{x}'(\tau)| d\tau \\ &= \frac{i}{4} \int_0^{2\pi} H_0^{(1)}(\kappa_1 |\mathbf{d}(t, \tau)|) \phi(\tau) |\mathbf{x}'(\tau)| d\tau, \end{aligned}$$

where  $\mathbf{d}(t, \tau) = \mathbf{y}(t) - \mathbf{x}(\tau)$ , for  $\mathbf{y} \in \Gamma_0$  and  $\mathbf{x} \in \Gamma_1$ .

We compute the Fréchet derivative by formally differentiating the kernel of the operator, resulting in

$$((S'_{101}(r_1; \phi))(q))(t) = \int_0^{2\pi} M(t, \tau) \phi(\tau) d\tau,$$

for the update  $q$  of the radial function  $r_1$ , with kernel

$$M(t, \tau) = \frac{i\kappa_1}{4} H_1^{(1)}(\kappa_1 |\mathbf{d}(t, \tau)|) \frac{\mathbf{d}(t, \tau) \cdot \mathbf{q}(\tau)}{|\mathbf{d}(t, \tau)|} |\mathbf{x}'(\tau)| + \frac{i}{4} H_0^{(1)}(\kappa_1 |\mathbf{d}(t, \tau)|) \frac{\mathbf{x}'(\tau) \cdot \mathbf{q}'(\tau)}{|\mathbf{x}'(\tau)|}$$

Since

$$\mathbf{q}'(\tau) = q'(\tau)(\cos \tau, \sin \tau) + q(\tau)(-\sin \tau, \cos \tau),$$

we decompose the kernel  $M$ , to the parts applied to  $q$  and its derivative, as follows

$$\begin{aligned} M(t, \tau) &= \left( \frac{i\kappa_1}{4} H_1^{(1)}(\kappa_1 |\mathbf{d}(t, \tau)|) \frac{\mathbf{d}(t, \tau) \cdot (\cos \tau, \sin \tau)}{|\mathbf{d}(t, \tau)|} |\mathbf{x}'(\tau)| \right. \\ &\quad \left. + \frac{i}{4} H_0^{(1)}(\kappa_1 |\mathbf{d}(t, \tau)|) \frac{\mathbf{x}'(\tau) \cdot (-\sin \tau, \cos \tau)}{|\mathbf{x}'(\tau)|} \right) q(\tau) \\ &\quad + \frac{i}{4} H_0^{(1)}(\kappa_1 |\mathbf{d}(t, \tau)|) \frac{\mathbf{x}'(\tau) \cdot (\cos \tau, \sin \tau)}{|\mathbf{x}'(\tau)|} q'(\tau). \end{aligned}$$

We approximate the updated radial function using trigonometric interpolation with  $2M + 1$  coefficients. We consider half collocation points concerning the direct problem and we add noise to the far-field data concerning the  $L^2$  -norm:

$$e_\delta^\infty = e^\infty + \delta \frac{\|e^\infty\|_2}{\|u\|_2} u, \quad h_\delta^\infty = h^\infty + \delta \frac{\|h^\infty\|_2}{\|v\|_2} v,$$

for a given noise level  $\delta$ , and complex-valued vectors  $u$  and  $v$ , with normally distributed random variables as components.

In the numerical example, the domain is bounded by the curves with radial functions

$$r_0 = 0.8, \quad \text{and} \quad r_1 = 0.7\sqrt{0.5\cos^2 t + 0.1\sin^2 t},$$

and we set  $\lambda = 1$  for the impedance function. The material parameters are  $\varepsilon_0 = \mu_0 = 1$ , in the exterior domain and  $\varepsilon_0 = \mu_0 = 5$ , in the interior domain. We consider measurements from two incident directions and we use  $n = 64$  and  $M = 2$ . In Fig (1), we present the reconstructions for  $\theta = \pi/4$  and  $\varphi = 0, \pi$ . The boundary is initially approximated by a circle with radius 0.4. The recovered curve is obtained after 20 and 12 iterations for exact and noisy data, respectively.

We observe that the reconstructions are satisfactory and stable with respect to noise. However, they depend on the initial guess.

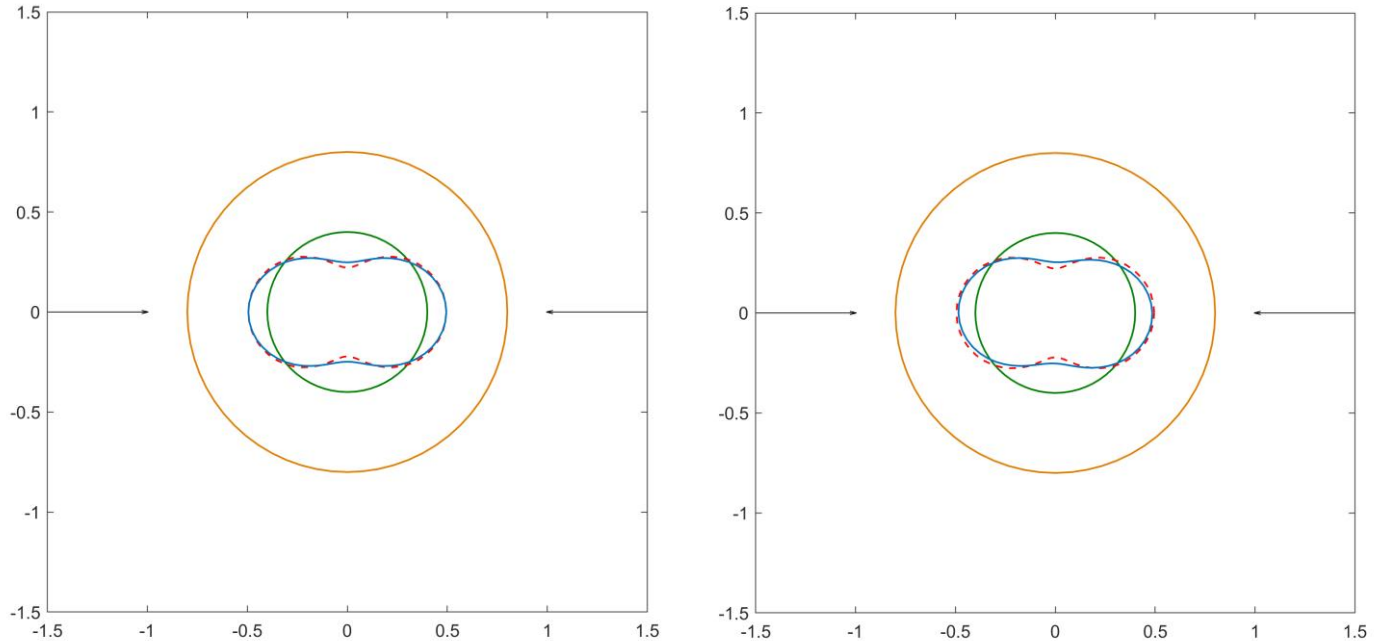


**Figure 1:** The reconstructed boundary curve (blue) for exact (left) and data with noise 4% (right) from two incident directions (arrows). The outer boundary (brown) and the initial guess (green) are both circles with different radii.

## Funding

Not applicable

## Conflict of Interest

The authors declare no conflict of interest.

## References

- [1] Colton D. Qualitative methods in inverse scattering theory. In: Engl HW, Louis AK, Rundell W, Eds. *Inverse problems in medical imaging and nondestructive testing*. Vienna: Springer; 1997. [https://doi.org/10.1007/978-3-7091-6521-8\\_4](https://doi.org/10.1007/978-3-7091-6521-8_4)
- [2] Kress R. *Linear integral equations*. vol. 82, 3rd ed. New York, NY: Springer; 2014. <https://doi.org/10.1007/978-1-4614-9593-2>
- [3] Kress R. A collocation method for a hypersingular boundary integral equation via trigonometric differentiation. *J Integral Equations Appl*. 2014; 26: 197-213. <https://doi.org/10.1216/JIE-2014-26-2-197>
- [4] Yousif HA, Köhler S. Scattering by two penetrable cylinders at oblique incidence I The analytical solution. *J Opt Soc Am A*. 1988; 5(7): 1085-96. <https://doi.org/10.1364/JOSAA.5.001085>
- [5] Wait JR. Scattering of a plane wave from a circular dielectric cylinder at oblique incidence. *Can J Phys*. 1955; 33: 189-95. <https://doi.org/10.1139/p55-024>
- [6] Nakamura G, Wang H. The direct electromagnetic scattering problem from an imperfectly conducting cylinder at oblique incidence. *J Math Anal Appl*. 2013; 397: 142-55. <https://doi.org/10.1016/j.jmaa.2012.07.049>
- [7] Wang H, Nakamura G. The integral equation method for electromagnetic scattering problem at oblique incidence. *Appl Num Math*. 2012; 62: 860-73. <https://doi.org/10.1016/j.apnum.2012.02.006>
- [8] Gintides D, Mindrinos L. The direct scattering problem of obliquely incident electromagnetic waves by a penetrable homogeneous cylinder. *J Integral Equations Appl*. 2016; 28: 91-122. <https://doi.org/10.1216/JIE-2016-28-1-91>
- [9] Gintides D, Mindrinos L. The inverse electromagnetic scattering problem by a penetrable cylinder at oblique incidence. *Appl Analysis*. 2019; 98: 781-98. <https://doi.org/10.1080/00036811.2017.1402891>

- [10] Mindrinos L. The electromagnetic scattering problem by a cylindrical doubly connected domain at oblique incidence: the direct problem. *IMA J Appl Math.* 2019; 84: 292-311. <https://doi.org/10.1093/imamat/hxy059>
- [11] Kress R, Rundell W. Nonlinear integral equations and the iterative solution for an inverse boundary value problem. *Inverse Probl.* 2005; 21: 1207-23. <https://doi.org/10.1088/0266-5611/21/4/002>
- [12] Johansson T, Sleeman BD. Reconstruction of an acoustically sound-soft obstacle from one incident field and the far-field pattern. *IMA J Appl Math.* 2007; 72: 7296-112. <https://doi.org/10.1093/imamat/hxl026>
- [13] Altundag A, Kress R. On a two-dimensional inverse scattering problem for a dielectric. *Appl Analysis.* 2012; 91: 757-71. <https://doi.org/10.1080/00036811.2011.619981>
- [14] Chapko R, Gintides D, Mindrinos L. The inverse scattering problem by an elastic inclusion. *Adv Comput Math.* 2017; 44: 1-24. <https://doi.org/10.1007/s10444-017-9550-z>
- [15] Lee K-M. Inverse scattering problem from an impedance crack via a composite method. *Wave Motion.* 2015; 56: 43-51. <https://doi.org/10.1016/j.wavemoti.2015.02.002>